RECORDSOF CHEMICAL SCIENCES

# Adsorption of Cadmium and Lead Ions on Activated Carbon prepared from Blended Bones of Cow and Goat

*Fatima Lawal*, Kamaluddeen Suleiman Kabo, and Sadiq Sani*

***https://doi.org/10.33003/frscs_2025_0401/10***

**Accepted**: 21th March, 2025
**Published**: 26th April, 2025

*1. Department of Chemistry, Federal University Dutsin-Ma, P.M.B 5001, Katsina State,*

**Corresponding Author:*
*Fatima Lawal*
*falawal@fudutsinma.edu.ng*

**FRsCS Vol. 4 No. 1 (2025) Official Journal of Dept. of Chemistry, Federal University of Dutsin-Ma, Katsina State. http://rscs.fudutsinma.edu.ng**

***ISSN (Online): 2705-2362***
***ISSN (Print): 2705-2354***

## Abstract

The study aims to investigate the potential of activated carbon from blended bones of cow and goat for the removal of lead and cadmium ions from wastewater. Bone samples of cow and goat were collected from Dustin-Ma old market, Katsina State, and washed with deionized water to remove contaminants before drying in an oven at 110°C for 24 h. The bones were mechanically ground into powder, carbonized in a muffle furnace at 700°C for 3 hrs, and sieved with a 300 µm sieve to obtain uniform particles. The carbon (50 g) was activated with concentrated hydrochloric acid (10 ml) for 4 h and washed with deionized water to a neutral pH. The adsorbent was characterized by Fourier-Transform Infrared Spectroscopy (FTIR), and Scanning Electron Microscope (SEM). The adsorption study was performed using Box-Behnken Design (BBD) to optimize the variables affecting the removal of metal and the response was determined using AAS. The adsorption isotherms were studied using the Langmuir and Freundlich models. The FTIR showed adsorption peaks of aldehyde, amide, hydroxyl, and carboxylic functional groups which aided the adsorption process. The activation of the bones impacted the surface morphologies compared to the raw bones, revealing a large surface area favoring the adsorption of the metal ions in the wastewater. The predicted maximum absorption for Cd2+ ion using an adsorbent dosage of 2.5 g, contact time of 20 min, adsorbate concentration of 10 ppm, and agitation speed of 274.98 rpm was 99.38%, while the maximum adsorption efficiency for Pb2+ ion using an adsorbent dosage of 2.5 g, contact time of 20 min, adsorbate concentration of 13.43 ppm, and agitation speed of 270.59 rpm was 98.03%. The linearized equilibrium data and the metal ions adsorption both obeyed the Langmuir and Freundlich models. R2 values of the Langmuir isotherm were 0.9823 for Cd2+ and 0.9725 for Pb2+ whereas Freundlich isotherm has R2 values of 0.9772 for Cd2+ and 0.9881 for Pb2+, indicating homogenous distribution. Conclusively, a blend of chemically activated bones of cow and goat bones can serve as an alternative low-cost adsorbent for the removal of cadmium and lead ions from wastewater.

**Keywords**: Adsorption, Bones, wastewater, Cadmium. Isotherms, low-cost

## Introduction

Heavy metals are environmental pollutants that can come from a variety of sources, such as lead in gasoline, industrial effluents, metal purification, ore smelting, nuclear fuel preparation, and electroplating (Saha et al., 2021). The heavy metals seep into surface water, subsurface water, and soil (Saha et al., 2020). Numerous countries, Nigeria included, have established organizations tasked with preventing environmental deterioration. For example, the National Environmental Standards and Regulation Enforcement Agency (NESREA) exists in Nigeria. Its responsibilities include passing laws that have been delegated to it by an authorizing body and carrying them out. Additionally, it guarantees that industrial wastes are processed to eliminate dangerous chemicals before being released into the environment or bodies of water like lakes, rivers, etc. (Kaluderovic et al., 2017). Consequently, a great deal of research has been done on the removal of heavy metals through ion exchange, reverse osmosis, chemical precipitation, electro-dialysis, electrolytic extraction, and coagulation techniques (Yilmaz et al., 2018). Nevertheless, many of these are too costly or unable to achieve treatment goals. Adsorption,

on the other hand, has been demonstrated to be a potentially workable alternative, with activated carbon adsorption being the most widely used method (Fanning *et al.,* 2021).

Activated carbon is currently considered a universal adsorbent for the removal of pollutants from contaminated water due to its high surface area, high adsorption capacity, fast kinetics, and relatively easy regeneration (Sathishkumar *et al*., 2012). Activated carbon is a carbonaceous material with high porosity that can be applied in the treatment of various wastewater for a variety of contaminants. It is necessary, however, to research and develop activated carbons of low cost and with alternative materials for use in the control of water pollution (Wang *et al*., 2010). The ease of obtaining activating carbon is also a positive factor since any materials with a high concentration of fixed carbon can be activated, for instance, pine knots, eucalyptus, coconut bark, palm bark, fruit pips, waste oil, and animal bone.

Several studies have been reported on lead and cadmium adsorption with activated carbon produced from alternative materials such as cashew nuts (Senthil Kumar *et al*., 2012), apricot seeds (Kobya *et al*., 2005), coconut shell (Sekar *et al*., 2004; Song *et al*., 2010), hazelnut bark (Imamoglu and Tekir, 2008), tamarind seeds (Acharya *et al*., 2009), grape seeds (Al Bahri *et al*., 2012), tobacco waste (Kilic *et al*., 2011) and rice husks (Yalçin and Sevinç, 2000; Liu *et al*., 2012). Research on activated carbon of animal origin is, generally, less common than studies on materials of plant origin, since their preparation requires long processing steps. Al-Asheh *et al.,* (2003) have presented results obtained for the adsorption of metals using chicken feathers. Although the use of animal bone blends such as goat and cow carbon to remove metal ions from wastewater is scarcely reported in life return. Hence, a need for research to look at the possibilities of its deployment in wastewater treatment, especially for the removal of heavy metals.

## MATERIALS AND METHODS

All the reagents used in this research were of analytical grade and were used without further treatment. The apparatus was thoroughly washed with detergents, rinsed with tap water, rinsed again with distilled and deionized water, and dried in an oven for 2 hrs. The instruments were also properly calibrated before being used.

### Sample collection

Bone samples were collected from Dustin-Ma old market, Katsina State, and washed with deionized water to remove contaminants before drying in an oven at 110℃ for 24 h.

### Pre-treatment and Activation of the bones

The bones were mechanically ground into powdered, sieved with a 300 µm sieve to obtain uniform particle size (Abdelbary *et al., 2021*) stored in polythene bags at room temperature for further use. The carbonization of cow and goat bones was achieved by weighing 2 g of the grounded sample in clean silica crucibles and heating it in an air-tight oven at 700℃ for 3 hrs (Youssef *et al., 2022*). The activation of bone charcoal was achieved using concentrated hydrochloric acid as an activating agent with a ratio of 10 ml per 50 g and a contact time of 4 hours. The carbons were washed with distilled water till a neutral medium (pH=7) was attained. This is done to remove the remains of acid, then filtered with the aid of a vacuum pump and dried at 100℃ in an oven for 2 hrs.

The powdered activated charcoal acquired was used for the adsorption analysis. (Arriagada *et al., 2021*).

**Box-Benhken Experimental Design**

The experimental design and statistical analysis were performed using the BBD of RSM because of its uniqueness in generating a higher-order surface response. An experimental design was conducted at three-level-four variable BBD. These independent variables are the initial concentration (A), agitation time (B), and agitation speed (C) operated at three levels (low, central, high) coded -1, 0, and +1 (Table 1a). Other variables, including light intensity, delivery volume, agitation speed, and oxygen pressure remained constant. A total of 17 experiments (N) were done based on the formula N = 2n + 2n + 5. Where n is the number of variables. The % D obtained from these experiments was processed using the upgraded Design Expert software DX 6.0.6 to obtain the predicted responses, response surface, and regression model for the adsorption.

**Table 1a:** The level factorial Box Benhken Design

| Variables | Units | Low (-1) | Middle (0) | High (+1) |
|---|---|---|---|---|
| Time (A) | Min | 20 | 60 | 100 |
| Concentration (B) | Ppm | 10 | 20 | 30 |
| Agitation Speed (C) | Rpm | 100 | 200 | 300 |

**Characterizations of Adsorbent**

Scanning electron microscopy (SEM) was used to investigate the influence of activation on porosity and also to study the physical surface morphology of the activated charcoal before and after adsorption. The scanning electron micrographs depict the illustrative morphology of the topographical microstructures of the adsorbent (Nwankwo *et al*., 2018). Fourier transform infrared spectroscopy (FTIR) analysis, the activated charcoal before and after absorption was subjected to an FT-IR spectrometer. The spectra were interpreted. The method used was adapted as described by Nwankwo *et al*. (2018)

## RESULTS AND DISCUSSION

**Fourier Transform Infrared (FTIR) Spectroscopy**

**Table 1**: Interpretation of FTIR peaks observed on (ACBC) and carbonized goat bone (CCBC) before adsorptions.

| S/N | Peaks ($cm^{-1}$) | Carbonized and activated (cow bones adsorbent) Functional group |
|---|---|---|
| | 663-683 | C-H aromatic bending |
| | 702- 875 | C-C vibrational Stretching bond |
| | 873-963 | C-C bending bond |
| | 1017-1087 | C-O in carboxylic acid |

| | |
|---|---|
| 1411-1458 | C-H deformation |
| 1508-1560 | C=O Aldehydes |
| 1637-1655 | C=C=C Stretching Vibration |
| 1978-1989 | C=C Stretching |
| 2013-2166 | O-H secondary cyclic alcohol |

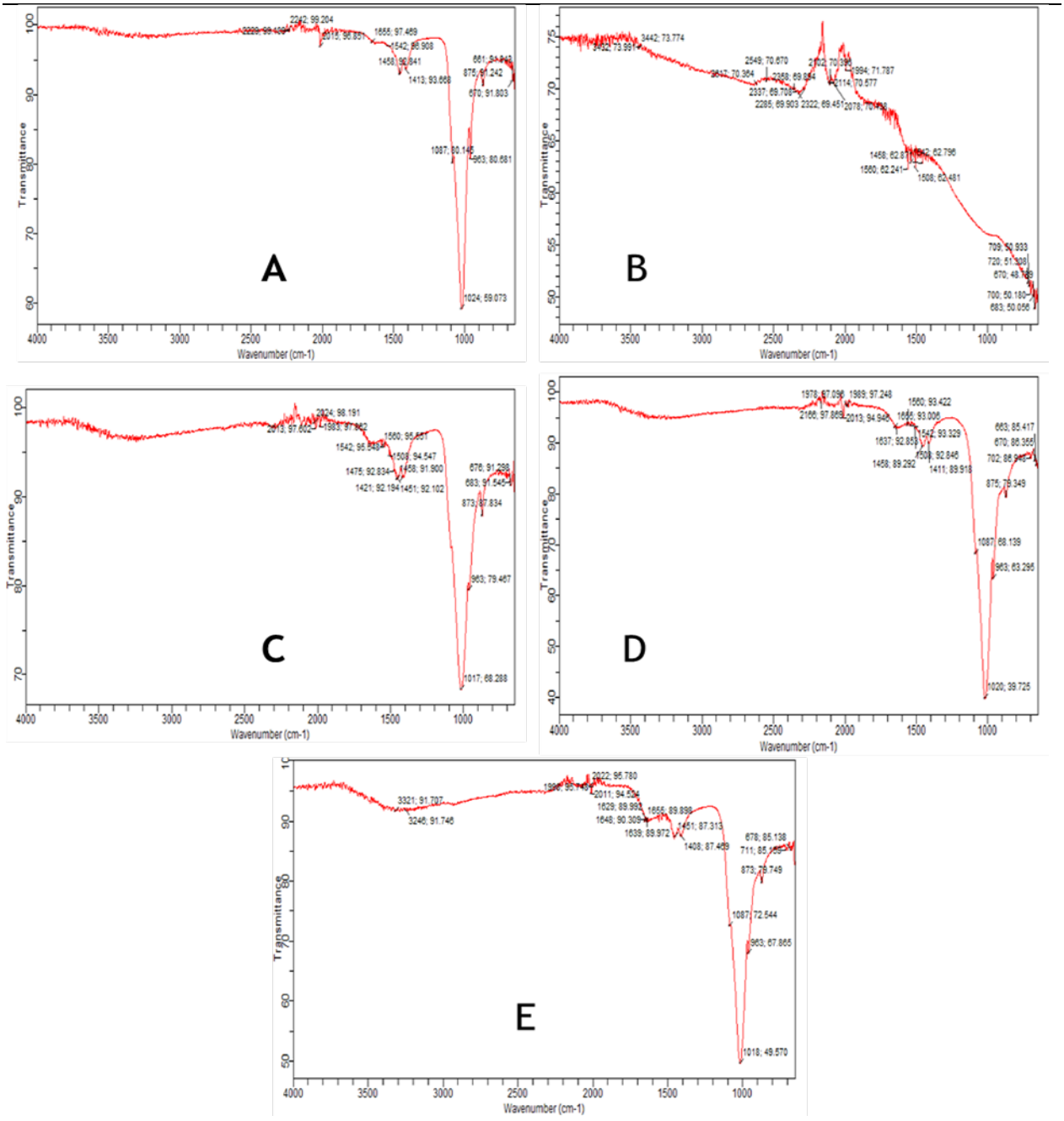


**Fig 1: A.** Carbonized cow bones before Adsorption **B.** Activated cow bones before Adsorption **C.** Carbonized goat bones before Adsorption **D.** Activated goat bones before Adsorption **E.** Blended cow and goat bones After Adsorption

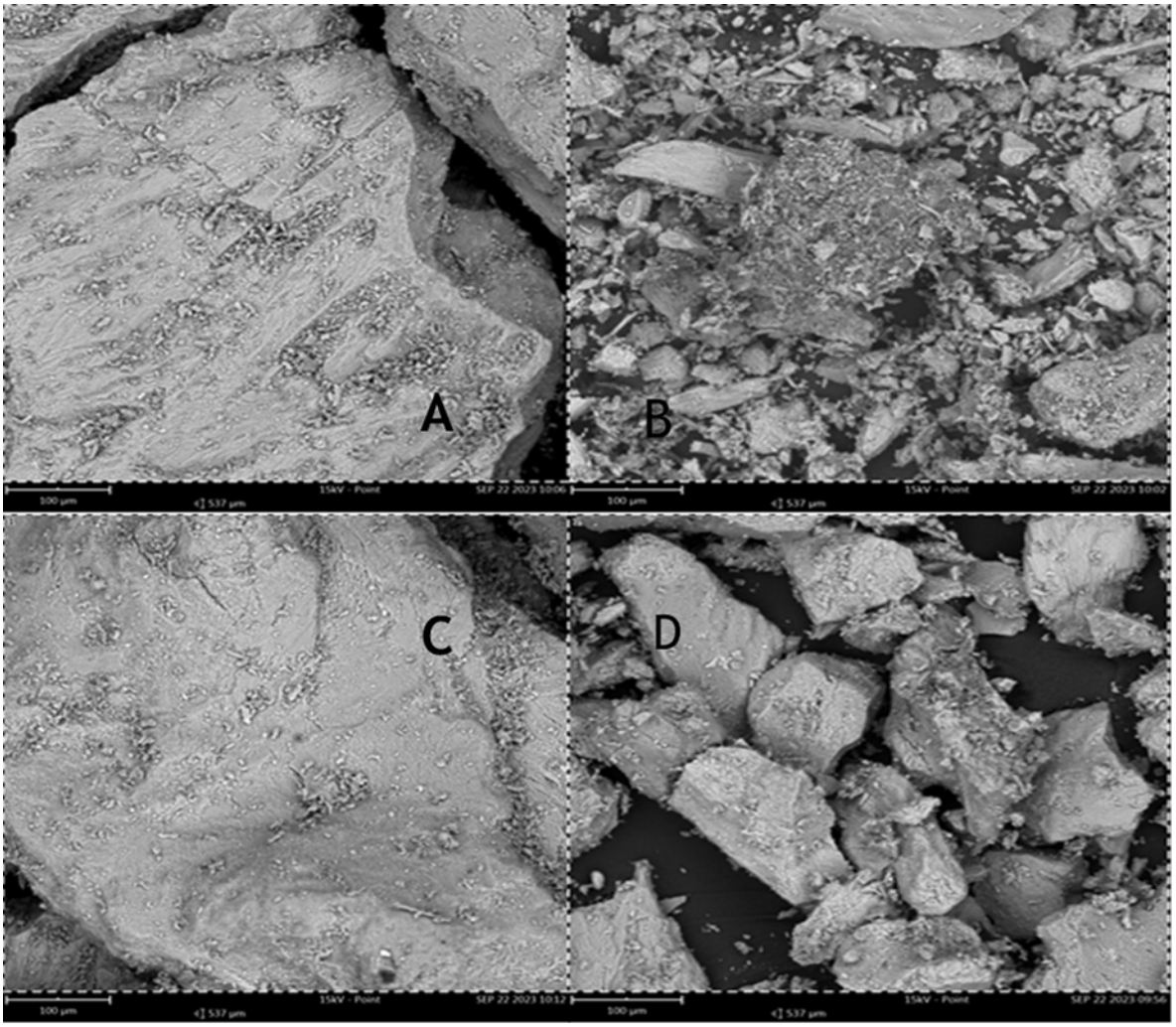


**Fig 2: A.** SEM Spectra Carbonized Cow Bones **B.** Activated Cow Bones Carbon Adsorbent **C**. SEM Spectra Carbonized Goat Bones **D**. Activated Goat Bones Carbon Adsorbent

The FTIR analysis of the adsorbents was carried out between 4000 – 100 $cm^{-1}$ revealing the vibrational frequency changes of the functional groups in the adsorbents. Table 1 shows FTIR spectra of activated cow bone (ACBC) and carbonized cow bone (CCBC), while Table 2 shows FTIR spectra of activated goat bone (AGBC) and carbonized goat bone (CGBC). Table 3 shows the FTIR spectra of blended cow and goat bone after adsorption, respectively.

**Table 2**: Interpretation of FTIR peaks observed on (ACBC) activated and carbonized goat bone (CCBC) before adsorptions

| Carbonized and activated (goat bones adsorbent) | |
|---|---|
| **S/N Peaks ($cm^{-1}$)** | **Functional group** |
| 661-683 | N-H and C-H rocking |
| 700- 720 | C-C Stretching |
| 875-963 | O-H bending |
| 1024-1024 | C-O in carboxylic acid |
| 1413-1458 | C-H deformation |
| 1508-1560 | C=C Stretching |
| 1655-1994 | C=C=C Stretching Vibration |
| 2015-2078 | C=C Stretching |
| 2102-2114 | O-H secondary cyclic alcohol |
| 2220-2285 | C-C Stretching |
| 3432-3442 | O-H Stretching |

**Table 3**: Interpretation of FTIR peaks observed on (ACBC) blended bone (CCBC) before adsorptions

| Blended bone bones adsorbent | |
|---|---|
| **S/N Peaks ($cm^{-1}$)** | **Functional group** |
| 678-711 | O-H and C-H stretching |
| 875-963 | O-H bending |
| 1018-1087 | C-O in carboxylic acid |
| 1408-1451 | C-H deformation |
| 1508-1560 | C=C Stretching |
| 1629-1639 | C=C=C Stretching Vibration |
| 1648-1998 | C=C Stretching |
| 2011-2022 | O-H secondary cyclic alcohol |
| 2220-2285 | C-C Stretching |
| 3246-3321 | O-H Stretching monomeric alcohol |

The results obtained from Table 1 show FT-IR spectra of activated and carbonized cow borne (ACBC) before, while Table 2 shows FT-IR spectra of activated and carbonized goat bone (ASBC) adsorption, respectively. In Table 1, the peaks observed at 676.91 – 683.91 $cm^{-1}$ indicate of existence of a bonded hydroxyl group. The peaks around

702, 873, 875, 963, 1020, 1411 and 1458 cm$^{-1}$ were assigned to C-H, C=O, OH, and aromatic ring stretching, respectively. In Table 2, the peaks observed at 3442, 2617, 2549, 2322, 2285,1542, 1994, and 1508 indicate the presence of OH, C=O, C-H, and aromatic rings, respectively. The additional and oversight peaks and changes in vibrational frequencies after the adsorption of metal ions indicate that adsorption has taken place (Slimani *et al*., 2013). In Table 3, the peaks observed at 678, 711, 873, 963, 1018, 1087, 1408, and 1451 cm$^{-1}$ were O-H and C-H stretching vibrational bonds indicating the presence of hydroxyl and alkyl groups. The peaks around 1629, 1639, 1648, 1998, 2011, 2022, 3246, and 3321 cm$^{-1}$ were assigned C=O Aldehyde, ketone, carboxylic acid, esters, phenol, and alcohol respectively.

**Surface Morphology**

The surface morphology of the adsorbents before and after adsorption was observed by SEM for ACBC in Figures 1, and 2; AGBC in Figures 3, and 4.

**Scanning Electron Microscopy (SEM)**

The surface morphologies of the adsorbents were observed by SEM in Figures 1, 2, 3, and 4 for ACBC and CCBC charcoals, respectively. It is a result of the presence of quite a lot of particles in coals. Figures 3 and 4 are for AGBC and CCBC. The results obtained from SEM show many pores were created due to the breakage in the surface of the adsorbents. It shows little porosity for both adsorbents. This supports the adherence of the metal ion molecules. A similar observation was made in Figures 3 and 4 for AGBC charcoals ACBC. These changes in morphologies were in good agreement with the literature for various materials (Dawlet *et al*., 2013; Slimani *et al*., 2014).

**Adsorption Experiments**

The experiments were carried out using the method according to Saha et al. *(*2021). Exactly 50.0cm$^3$ of cadmium/lead solution was measured into polythene bottles and 2.5g adsorbent was transferred into these bottles. The mixtures in 250 ml volumetric flask bottles were agitated reciprocating shaker at 200 rpm for 3 h and left undisturbed on the desk for 24 h to allow the system to equilibrate. After 24 h, the mixture was filtered through a Whatman filter paper into another 100 cm$^3$ polyethylene bottle. The concentration of the adsorbed metal ion in the filtrate after the adsorption process was determined using AAS (Światkowski *et al.,* 2017). The amount of the metal adsorbed was calculated using the equation

$$q_e = \frac{V(C_o - C_e)}{1000\ m}$$

where $q_e$ is the amount of adsorbate ion adsorbed in milligrams per gram of the adsorbent.

$C_o$ is the initial concentration of the metal ion before the adsorption process, while

$C_e$is the equilibrium concentration of the metal ion in the filtrate after the adsorption process,

m is the mass of the adsorbent and V is the volume of the solution in cm$^3$

The equation that gives percentage of metal ion removal by the adsorbent is given by:

$$\% \text{ Adsorbed} = \frac{(C_o - C_e)}{C_o} \times 100$$

$C_o$ is the initial concentration of the metal ion before the adsorption process

$C_e$ is the equilibrium concentration of the metal ion in the filtrate after the adsorption process

**Optimization Scheme**

The experimental and predicted response efficiency for $Cd^{2+}$ ions obtained are shown in Table 5. The predicted responses ($D_{cal}$ %) fit the generic, second-order polynomial mode in eq. (17). The experimental optimum response efficiency (99.38%) was achieved at a contact time of 20 min, an adsorbent dosage of 2.5 g, and concentration of 10 ppm, agitation speed of 274.98 rpm. While $Pb^{2+}$ ion is shown in Table 6: The predicted responses ($D_{cal}$ %) fit the generic, second-order polynomial mode in eq. (17). The experimental optimum response efficiency (98.03%) was achieved at a contact time of 20 min, concentration of 13.43 ppm, and agitation speed of 270.59 rpm.

**Table 5: Experimental Design and Process of Optimization for Cadmium ion**

| Std | Run | Contact Time (min) | Concentration (ppm) | Agitation speed (rpm) | Response Efficiency (%) |
|---|---|---|---|---|---|
| **12** | 1 | 60 | 30 | 300 | 97.38 |
| **16** | 2 | 60 | 20 | 200 | 98.23 |
| **7** | 3 | 20 | 20 | 300 | 99.18 |
| **3** | 4 | 20 | 30 | 200 | 96.23 |
| **11** | 5 | 60 | 10 | 300 | 95.63 |
| **9** | 6 | 60 | 10 | 100 | 94.48 |
| **13** | 7 | 60 | 20 | 200 | 99.33 |
| **14** | 8 | 60 | 20 | 200 | 98.38 |
| **8** | 9 | 100 | 20 | 300 | 97.1 |
| **2** | 10 | 100 | 10 | 200 | 94.6 |
| **17** | 11 | 60 | 20 | 200 | 98.5 |
| **4** | 12 | 100 | 30 | 200 | 99.9 |
| **1** | 13 | 20 | 10 | 200 | 96.36 |
| **5** | 14 | 20 | 20 | 100 | 96.38 |
| **6** | 15 | 100 | 20 | 100 | 96.38 |
| **10** | 16 | 60 | 30 | 100 | 96.23 |
| **15** | 17 | 60 | 20 | 200 | 94.48 |

**Table 6: Experimental Design and Optimization for $Pb^{2+}$ ion**

| Std | Run | Contact time (min) | Concentration (ppm) | Agitation speed (rpm) | Adsorption Efficiency (%) |
|---|---|---|---|---|---|
| **12** | 1 | 60 | 30 | 300 | 98.41 |
| **16** | 2 | 60 | 20 | 200 | 98.1 |
| **7** | 3 | 20 | 20 | 300 | 99.19 |
| **3** | 4 | 20 | 30 | 200 | 98.56 |
| **11** | 5 | 60 | 10 | 300 | 98.91 |
| **9** | 6 | 60 | 10 | 100 | 99.9 |
| **13** | 7 | 60 | 20 | 200 | 98.1 |
| **14** | 8 | 60 | 20 | 200 | 99.3 |
| **8** | 9 | 100 | 20 | 300 | 99.15 |
| **2** | 10 | 100 | 10 | 200 | 99.74 |
| **17** | 11 | 60 | 20 | 200 | 97.2 |
| **4** | 12 | 100 | 30 | 200 | 92.94 |
| **1** | 13 | 20 | 10 | 200 | 97.86 |
| **5** | 14 | 20 | 20 | 100 | 99.65 |
| **6** | 15 | 100 | 20 | 100 | 97.5 |
| **10** | 16 | 60 | 30 | 100 | 94.49 |
| **15** | 17 | 60 | 20 | 200 | 95.42 |

**Table 7**: Analysis of variance (ANOVA) of the fitted quadratic equations for the adsorption of $Cd^{2+}$ion.

| **Response:** | **Responses Efficiency** | | **Cadmium** | | | |
|---|---|---|---|---|---|---|
| **ANOVA for Response Surface Quadratic Model** | | | | | | |
| **Analysis of variance table [Partial sum of squares]** | | | | | | |
| **Source** | Sum of Squares | DF | Mean Square | F Value | Prob > F | |
| **Model** | 34.88036 | 9 | 3.875595 | 2752.833 | < 0.0001 | Significant |
| **A** | 0.6728 | 1 | 0.6728 | 477.8894 | < 0.0001 | |
| **B** | 5.040313 | 1 | 5.040313 | 3580.131 | < 0.0001 | |
| **C** | 4.977013 | 1 | 4.977013 | 3535.169 | < 0.0001 | |
| **A2** | 1.626367 | 1 | 1.626367 | 1155.208 | < 0.0001 | |
| **B2** | 1.056846 | 1 | 1.056846 | 750.6772 | < 0.0001 | |
| **C2** | 2.667857 | 1 | 2.667857 | 1894.977 | < 0.0001 | |
| **AB** | 18.19023 | 1 | 18.19023 | 12920.5 | < 0.0001 | |
| **AC** | 0.801025 | 1 | 0.801025 | 568.9675 | < 0.0001 | |
| **BC** | 0.0081 | 1 | 0.0081 | 5.753425 | 0.0476 | |
| **Residual** | 0.009855 | 7 | 0.001408 | | | |
| **Lack of Fit** | 0.009175 | 3 | 0.003058 | 17.9902 | 0.0087 | Significant |
| **Pure Error** | 0.00068 | 4 | 0.00017 | | | |
| **Cor Total** | 34.89021 | 16 | | | | |
| **The Model F-value of 2752.83 implies the model is significant. There is only a 0.01% chance that a "Model F-Value" this large could occur due to noise.** | | | | | | |

**Table 8**: Analysis of variance (ANOVA) of the fitted quadratic equations for the adsorption of for the quadratic $Pb^{2+}$ ion.

| **Response:** | **Responses Efficiency** | | **Lead (pb)** | | | |
|---|---|---|---|---|---|---|
| **ANOVA for Response Surface Quadratic Model** | | | | | | |
| **Analysis of variance table [Partial sum of squares]** | | | | | | |
| **Source** | Sum of Squares | DF | Mean Square | F Value | Prob > F | |
| **Model** | 51.47856 | 9 | 5.71984 | 4.457285 | 0.0308 | Significant |
| **A** | 4.395613 | 1 | 4.395613 | 3.425358 | 0.1066 | |
| **B** | 18.03001 | 1 | 18.03001 | 14.0502 | 0.0072 | |
| **C** | 2.1218 | 1 | 2.1218 | 1.65345 | 0.2394 | |
| **A2** | 0.373912 | 1 | 0.373912 | 0.291377 | 0.6061 | |
| **B2** | 1.762564 | 1 | 1.762564 | 1.373509 | 0.2795 | |
| **C2** | 3.804001 | 1 | 3.804001 | 2.964334 | 0.1288 | |
| **AB** | 14.0625 | 1 | 14.0625 | 10.95845 | 0.0129 | |
| **AC** | 1.113025 | 1 | 1.113025 | 0.867344 | 0.3827 | |
| **BC** | 6.027025 | 1 | 6.027025 | 4.696665 | 0.0669 | |
| **Residual** | 8.982795 | 7 | 1.283256 | | | |
| **Lack of Fit** | 0.683275 | 3 | 0.227758 | 0.109769 | 0.9499 | not significant |
| **Pure Error** | 8.29952 | 4 | 2.07488 | | | |
| **Cor Total** | 60.46135 | 16 | | | | |

The Model F-value of 4.46 implies the model is significant. There is only a 3.08% chance that a "Model F-Value" this large could occur due to noise.

However, the closeness of the values between the experimental and predicted response is a clear indication of the accuracy of the model. Similarly, this good correlation is attested to the linear normal plot of residual (Fig. 5). The majority of the points on the normal probability plot lie roughly on a straight line, so it can be conclude that are real and differ markedly from noise.

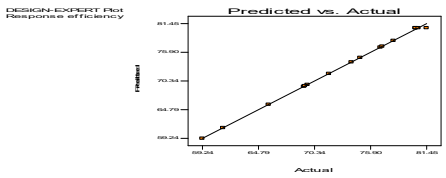


**Fig. 5**. Linear normal plot of residual

Analysis of variance (ANOVA) was performed in order to check the model accurately by evaluating the sum of squares, degree of freedom, mean square, F-value, and p-value, and the results are shown in Table 6. From the Table, the model value of 13.89 implies model significance and that there is only a 0.03 % chance of a noisy model F-value. The quality of the developed model is high given that $R^2$ = 0.9815. This implies that 98 % of the variations in the response efficiency were explained by the independent variables within the studied range. The lack of fit value of 0.62 is not significant relative to the pure error when the p-value is 0.7621 (more than 0.05) which shows good predictability of the model. Meanwhile, the significance of the model terms is proven by the small p-value (less than 0.0001). Other model terms are insignificant as their p-values were greater than 0.1000. From Table 7, the coefficient of variance (C.V. = 1.14) is low indicating high precision and good reliability of the experimental values. Adequate precision measure of 33.17, which is well above 4 indicates an adequate signal. The regression model demonstrates a good relationship between independent variables, as both $R^2$ (0.9786) was close to 1. In the study, the p-values of the major parameters (A and C) influencing the percentage removal of $cd^{2+}$ are significant

.

**Table 9**: Analysis of variance results for the quadratic model

| Parameter | Value |
|---|---|
| Standard deviation | 3.01 |
| Mean | 82.72 |
| Coefficient of variance (CV, % ) | 1.14 |
| Coefficient of determination ($R^2$) | 0.979 |
| Adjusted $R^2$ | 0.969 |
| Predicted $R^2$ | 0.798 |
| Adequate precision | 33.17 |

To validate the quadratic model obtained in this study, runs were individually performed and compared to the predicted results. (Tables 5 and 6). The experimental results were very close to the predicted values (99.38 %) and (98.03%) confirming the reliability of the BBD. Fig.7 (a) shows a three-dimensional response surface and contour plot of the influence $Pb^{2+}$ ion and initial concentration, contact time at constant agitation speed. The removal percentage increased proportionally with an increase in response efficiency dosage due to enhancement in the generation of hydroxyl radicals. Fig. 7 (b). From the response surface and contour plot, the response efficiency was low at acidic pH value due to the loss of $pb^{2+}$ ion perhaps, whereas at an alkaline medium hydroxyl radicals played a positive role in the removal of waste as earlier observed in the case of other organic contaminants. Lastly, Fig 7 (c) shows the effect of contact time and agitation speed at a constant concentration. However, the

response efficiency reduced with increasing concentration.

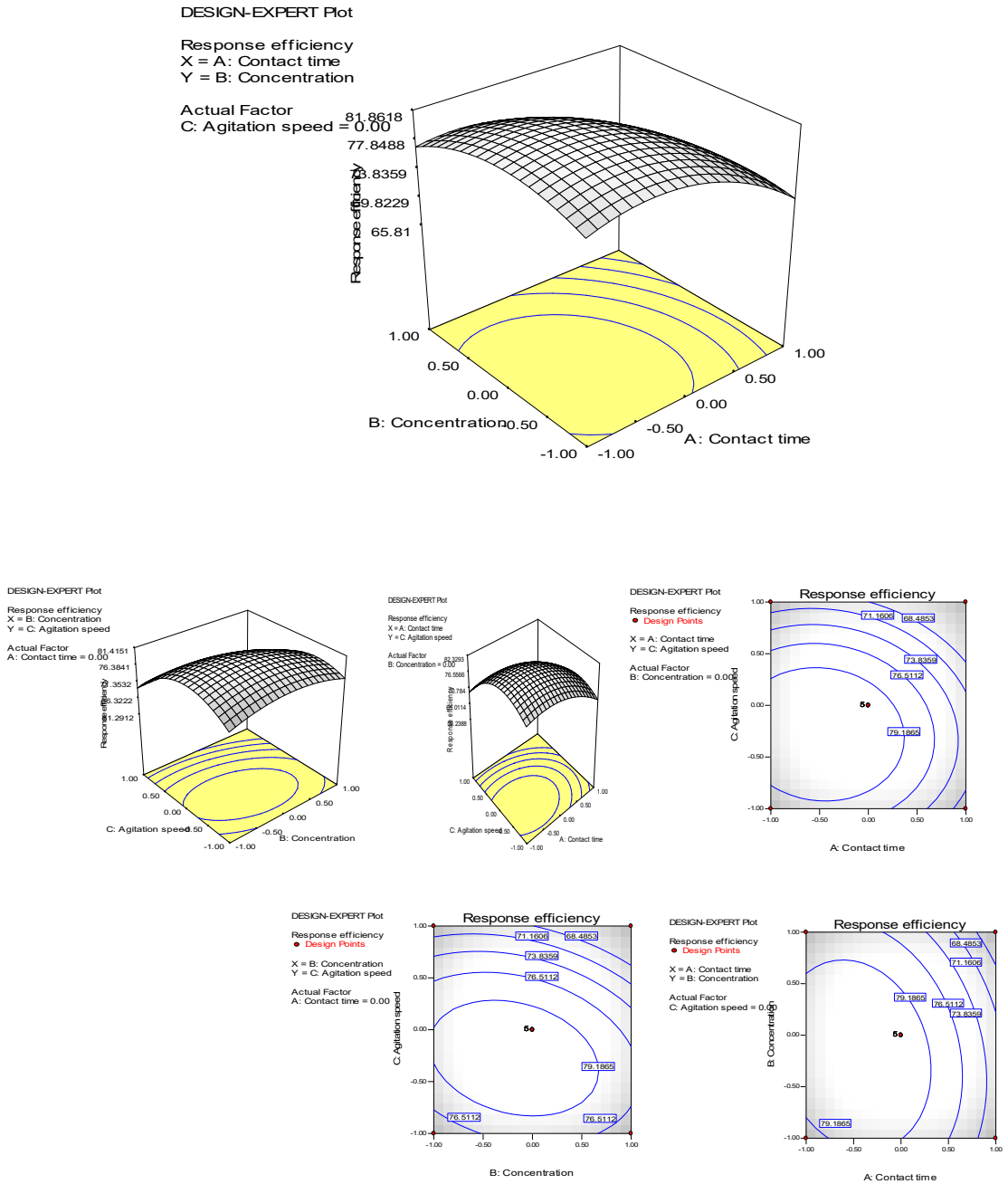


**Fig. 7.** The 3D response surfaces and contour plot for (a) contact time (b) concentration (c)

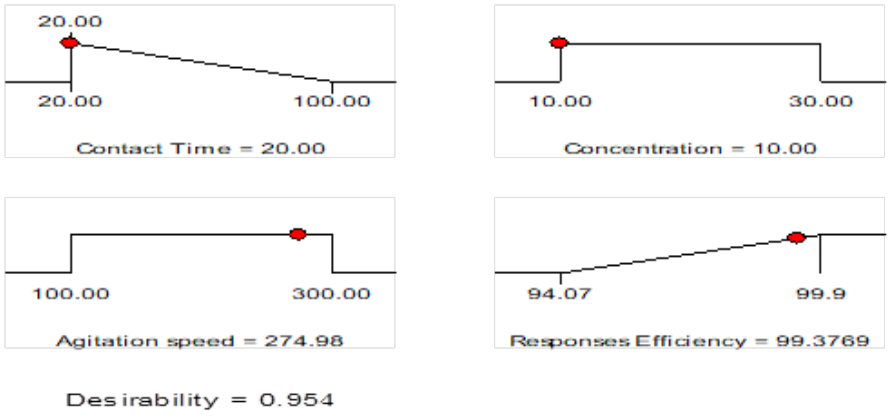


**Fig**. 8. Optimum Condition responses Parameters for Cadmium ($Cd^{2+}$) ion

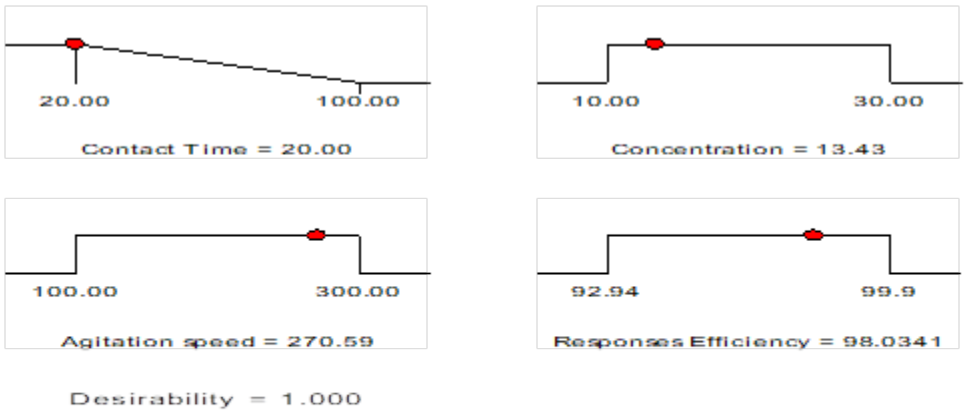


**Fig**. 9. Optimum Condition responses Parameters for Cadmium ($Pb^{2+}$) ion

**Optimization**:

In Figures 7 and 8 the optimal conditions for removing $Cd^{2+}$ and $Pb^{2+}$, which have been designed and predicted by the software, can be seen. In this figure, the effect of different factors on the metal's removal response and the optimal values of each factor for metal removal in the ideal state are specified. Based on the results obtained from the figure, the highest removal percentage of 99.38 and 99.03% is predicted. The predicted results were close to the experimental results and disclosed that the model designed to remove the metals is a suitable model.

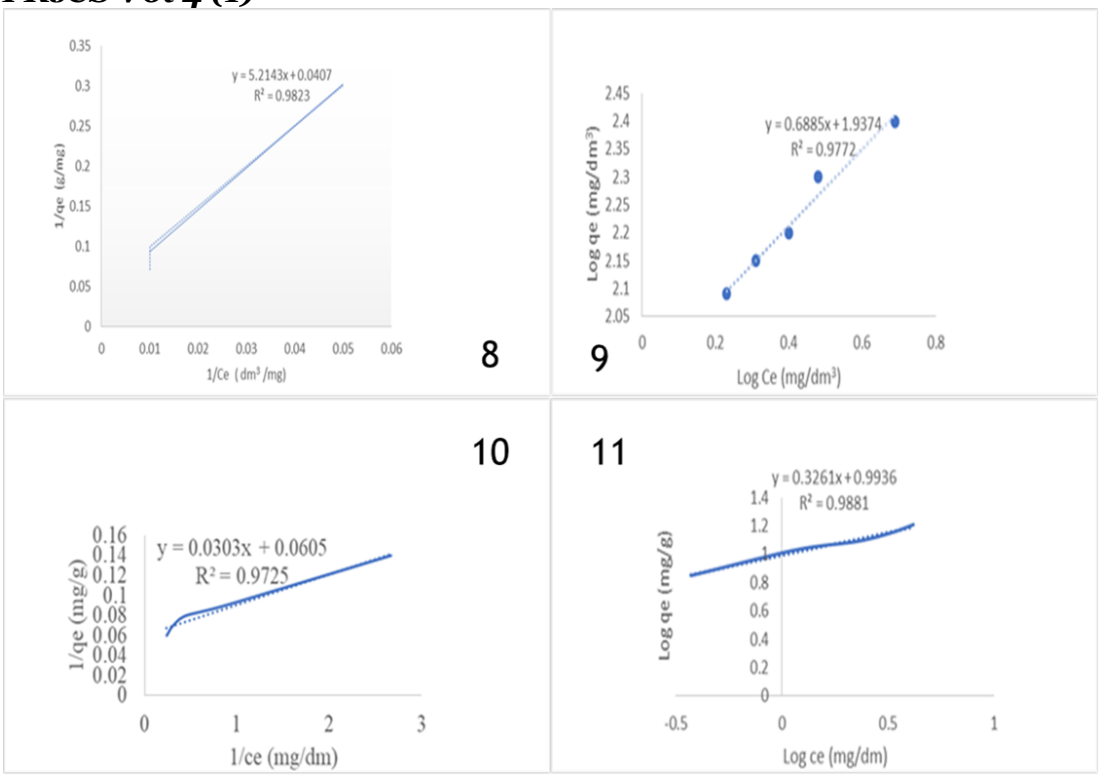


**Fig. 8, 9, 10, 11:** Langmuir Adsorption Isotherm for $Cd^{2+}$ Adsorption; Freundlich Adsorption Isotherm for $Cd^{2+}$ Adsorption; Langmuir Adsorption Isotherm for $Pb^{2+}$ Adsorption; Freundlich Adsorption Isotherm for $Pb^{2+}$ Adsorption

**Adsorption isotherms mechanism**

Among the many adsorption isotherms used to model the amount of solute adsorbed per unit of adsorbent as a function of equilibrium concentration in the bulk solution Freundlich and Langmuir were evaluated. In this study, consistency was only obtained with both Freundlich and Langmuir isotherms, and their parameters for cadmium and lead adsorption are presented in Table 10. It would be seen from the table that the Freundlich and Langmuir isotherms are linear with correlation coefficient $R^2$ in the range of 0.9881, 0.9823, 0.9772, 0.925 –1.000. Agreement with both Langmuir and Freundlich.

**Table 10:**Langmuir and Freundlich Constant for Cadmium and Lead

| **Metals** | **Langmuir Constant** | | | **Freundlich Constant** | | |
|---|---|---|---|---|---|---|
| | $q_{max}$ (mg/g) | b($dm^3$/mg) | $R^2$ | **1/n** | $K_f$($dm^3$/mg) | $R^2$ |
| **Cadmium** | 24.75 | 0.0078 | 0.9823 | 1.452 | 86.27 | 0.9772 |
| **Lead** | 16.53 | 1.997 | 0.9725 | 3.067 | 9.797 | 0.9881 |

**Table 11:** The $R_L$ Separation Factor of Adsorption of $Cd^{2+}$ on Blended animal-bones Activated Carbon

| $q_{max}$ | qmax($m^3$/kg) | Initial Conc. (mg/$dm^3$) | $R_L$ |
|---|---|---|---|
| | | 20 | 0.2057 |
| | | 40 | 0.1147 |
| **24.75** | 0.19305 | 60 | 0.0795 |
| | | 80 | 0.0608 |
| | | 100 | 0.0492 |
| | | 120 | 0.0414 |

**Table 12:** The $R_L$ Separation Factor of Adsorption of $Pb^{2+}$ on Blended animal-bones Activated Carbon

| $q_{max}$ | qmax($m^3$/kg) | Initial Conc. (mg/$dm^3$) | $R_L$ |
|---|---|---|---|
| | | 20 | 0.0244 |
| | | 40 | 0.0124 |
| **16.53** | 0.19305 | 60 | 0.0083 |
| | | 80 | 0.0062 |
| | | 100 | 0.0050 |

## Conclusion

From the experimental observation, results, and discussion of this research work, it can be inferred that the blended animal bone sample used as activated carbon has these: It is a cheap, good alternative source for activated carbon production. It can be used as an adsorbent for the adsorption of the $Cd^{2+}$ and $Pb^{2+}$. The adsorption process is highly dependent on, contact time, agitation speed, and initial concentration. The adsorption capacity of activated carbon prepared from blended animals' bone with both acid and base activators has a comparable strength adsorption rate which is higher than commercial activated carbon. It was observed that the trend of metal affinity for the activated surface was $Cd^{2+} > Pb^{2+}$. Activation of the two bone samples has improved the surface area of the bone. FTIR spectra analysis confirmed the presence of absorbance peaks of carboxyl, alkene, alkanol, amide, aldehyde, and alkyl functional groups. Thus, these functional groups are responsible for the adsorption of the selected metals. Additional functional groups and the large surface of the activated carbon can enhance the efficient adsorption of metal ions from wastewater.

## References

Abdelbary E.M., Youssef A.M., Samra S.E., Dowidar A.M. (2021). "Surface-properties of carbons obtained from polyvinyl-chloride". Ind. J. Chem. A. 30 (10): 839–843.

Abdelbary, E.M., Srinivasulu, A., Aruna, B., Banerjee, S., Sudarshan, M., Narayana, P.V.L. and Rao, A.D.P. (2021). Study of Heavy Metals Accumulation in

Leafy Vegetables of Ethiopia, OSR Journal of Environmental Science, Toxicology and Food Technology (IOSR-JESTFT), 11(5): 57-68

Acedo-Ramos M., Gomez-Serrano V., Valenzuella-Calahorro C., Lopez-Peinado A.J. (2023). "Oxydation of activated carbon in liquid phase. Study by FT-IR". Spectroscopy Letters. 26 (6): 1117–1137. Bibcode:2013SpecL.26.1117A. doi:10.1080/00387019308011598.

Aldana-Pérez A, Lartundo-Rojas L, Gómez R, Niño-Gómez ME (2022). "Sulfonic groups anchored on mesoporous carbon Starbons-300 and its use for the esterification of oleic acid". Fuel. 100: 128–138. doi: 10.1016/j.fuel.2012.02.025.

Arriagada R., Garcia R., Molina-Sabio M., Rodriguez-Reinoso F. (2017). "Effect of steam activation on the porosity and chemical nature of activated carbons from Eucalyptus globulus and peach stones". Microporous Mat. 8 (3–4): 123–130. doi:10.1016/s0927-6513(96)00078-8.

Beck S., Szymański G., Siedlewski J., Świątkowski A. (2022). "The characterizaíion of activated carbons with oxygen and nitrogen surface groups". Carbon. 35 (12): 1799–1810. Bibcode:1997Carbo..35.1799B. doi:10.1016/s0008-6223(97)00096-1.

Biniak S., Szymański G., Siedlewski J., Świątkowski A. (2017). "The characterizaíion of activated carbons with oxygen and nitrogen surface groups". Carbon. 35 (12): 1799–1810. Bibcode:1997Carbo..35.1799B. doi:10.1016/s0008-6223(97)00096-1.

Boudou J.P., Chehimi M., Broniek E., Siemieniewska T., Bimer J. (2023). "Adsorption of H2S or SO2 on an activated carbon cloth modified by ammonia treatment" (PDF). Carbon. 41 (10): 1999–2007. doi:10.1016/s0008-6223(03)00210-0. S2CID 53137987.

Bradley RH, Sutherland I, Sheng E (2016). "Carbon surface: Area, porosity, chemistry, and energy". Journal of Colloid and Interface Science. 179 (2): 561–569. Bibcode:2016JCIS..179..561B. doi:10.1006/jcis.2016.0250.

Budarin VL, Clark JH, Tavener SJ, Wilson K (2014). "Chemical reactions of double bonds in activated carbon: Microwave and bromination methods". Chemical Communications (23): 2736–7. doi:10.1039/B411222A. PMID 15568092.

Bueno A., Freitas B., Dekanski A. (2014). "Surface characterization of oxidized activated carbon cloth". Carbon. 35 (8): 1047–1052. Bibcode:1997Carbo..35.1047P. doi:10.1016/s0008-6223(97)00057-2.

Campbell, J.R., Rosier, R.N., Novotny, L. and Puzas, J.E. (2016). The association between environmental lead exposure and bone density in children, *Environmental Health Perspectives,* 112(11):1200-1203.

Choo P., Siedlewski J., Świątkowski A. (2019). "The characterizaíion of activated carbons with oxygen and nitrogen surface groups". Carbon. 35 (12): 1799–1810. Bibcode:1997Carbo..35.1799B. doi:10.1016/s0008-6223(97)00096-1.

Davidsson L, Clark JH, Tavener SJ, Wilson K (2023). "Chemical reactions of double bonds in activated carbon: Microwave and bromination methods". Chemical Communications (23): 2736–7. doi:10.1039/B411222A. PMID 15568092.

Diyuk VE, Zaderko AN, Grishchenko LM, Yatsymyrskiy AV, Lisnyak VV (2022). "Efficient carbon-based acid catalysts for the propan-2-ol dehydration". Catalysis Communications. 27: 33–37. doi:10.1016/j.catcom.2012.06.018.

Evans MJ, Halliop E, Liang S, MacDonald JA (2018). "The effect of chlorination on surface properties of activated carbon". Carbon. 36 (11): 1677–1682. Bibcode:2018Carbo..36.1677E. doi:10.1016/S0008-6223(98)00165-1.

Fanning P.E., Vannice M.A. (2018). "A DRIFTS study of the formation of surface groups on carbon by oxidation". Carbon. 31 (5): 721–730. Bibcode:1993Carbo..31..721F. doi:10.1016/0008-6223(93)90009-y.

Freitas B., Dekanski A. (2014). "Surface characterization of oxidized activated carbon cloth". Carbon. 35 (8): 1047–1052. Bibcode:1997Carbo..35.1047P. doi:10.1016/s0008-6223(97)00057-2.

George T., Sandle N.K. (2023). "Effect of different oxidizing agent treatments on the surface properties of activated carbons". Carbon. 37 (8): 1323–1332. Bibcode:2019Carbo..37.1323P. doi:10.1016/s0008-6223(98)00328-5.

Gibert E, Zaderko AN, Yatsymyrskiy AV, Lisnyak VV (2013). "Efficient carbon-based acid catalysts for the propan-2-ol dehydration". Catalysis Communications. 27: 33–37. doi:10.1016/j.catcom.2012.06.018.

Gomez-Serrano V., Acedo-Ramos M., Lopez-Peinado A.J., Valenzuela-Calahorro C. (1991). "Stability towards heating and outgassing of activated carbon oxidized in the liquid-phase". Thermochimica Acta. 176: 129–140. doi:10.1016/0040-6031(91)80268-n.

Greene H, Sheng E (2019). "Carbon surface: Area, porosity, chemistry, and energy". Journal of Colloid and Interface Science. 179 (2): 561–569. Bibcode:2016JCIS..179..561B. doi:10.1006/jcis.2016.0250.

Jaishankar, M., Mathew, B.B., Shah, M.S. and Gowda, K.R.S. (2014). Biosorption of Few Heavy Metal Ions Using Agricultural Wastes. Journal of Environment Pollution and Human Health, 2(1):1–6.

Janes I, Sheng E (2019). "Carbon surface: Area, porosity, chemistry, and energy". Journal of Colloid and Interface Science. 179 (2): 561–569. Bibcode:2016JCIS..179..561B. doi:10.1006/jcis.2016.0250.

Jarup, L. (20). 15Hazards of heavy metal contamination, *British Medical Bulletin*, 68: 167–182.

Jones K., Sandle N.K. (2021). "Effect of different oxidizing agent treatments on the surface properties of activated carbons". Carbon. 37 (8): 1323–1332. Bibcode:2019Carbo..37.1323P. doi:10.1016/s0008-6223(98)00328-5.

Khopkar AN, Boldyrieva OY, Kaňuchová M, Lisnyak VV (2014). "Fluoroalkylated Nanoporous Carbons: Testing as a Supercapacitor

Electrode". Applied Surface Science. 470: 882–892. doi:10.1016/j.apsusc.2018.11.141. ISSN 0169-4332. S2CID 105746451.

Manahan, S.E. (2023). Toxicological Chemistry and Biochemistry, CRC Press, Limited Liability Company (LLC), 3rd edition

Mapanda, F., Mangwayana, E.N., Nyamangara, J. and Giller, K.E. (2015). The effects of long-term irrigation using water on heavy metal contents of soils under vegetables. Agriculture, Ecosystem and Environment, 107:151-156.

Molina-Sabio M., Gonzalez M.T., Rodriguez-Reinoso F., Sepulveda-Escribano A. (2016). "Effect of steam and carbon dioxide activation in the micropore size distribution of activated carbon". Carbon. 34 (4): 505–509. Bibcode:1996Carbo..34..505M. doi:10.1016/0008-6223(96)00006-1.

Nansé G, Papirer E, Fioux P, Moguet F, Tressaud A (2017). "Fluorination of carbon blacks: An X-ray photoelectron spectroscopy study: III. Fluorination of different carbon blacks with gaseous fluorine at temperatures below 100 °C influence of the morphology, structure and physico-chemical characteristics of the carbon black on the fluorine fixation". Carbon. 35 (4): 515–528. Bibcode:2017Carbo..35..515N. doi:10.1016/S0008-6223(97)00003-1.

Papirer E, Lacroix R, Donnet JB, Nanse G, Fioux P (2014). "XPS Study of the halogenation of carbon black-part 1. Bromination". Carbon. 32 (7): 1341–1358. Bibcode:2014Carbo..32.1341P. doi:10.1016/0008-6223(94)90121-X.

Papirer EN, Lacroix R, Donnet JB, Nansé GR, Fioux P (2015). "XPS study of the halogenation of carbon black—Part 2. Chlorination". Carbon. 33 (1): 63–72. Bibcode:2015Carbo..33...63P. doi:10.1016/0008-6223(94)00111-C.

Paul L, Clark JH, Tavener SJ, Wilson K (2015). "Chemical reactions of double bonds in activated carbon: Microwave and bromination methods". Chemical Communications (23): 2736–7. doi:10.1039/B411222A. PMID 15568092.

Polovina M., Babic B., Kaluderovic B., Dekanski A. (2017). "Surface characterization of oxidized activated carbon cloth". Carbon. 35 (8): 1047–1052. Bibcode:1997Carbo..35.1047P. doi:10.1016/s0008-6223(97)00057-2.

Pradhan B.K., Sandle N.K. (2019). "Effect of different oxidizing agent treatments on the surface properties of activated carbons". Carbon. 37 (8): 1323–1332. Bibcode:2019Carbo..37.1323P. doi:10.1016/s0008-6223(98)00328-5.

Radkevich VZ, Senko TL, Wilson K, Grishenko LM, Zaderko AN, Diyuk VY (2018). "The influence of surface functionalization of activated carbon on palladium dispersion and catalytic activity in hydrogen oxidation". Applied Catalysis A: General. 335 (2): 241–251. doi:10.1016/j.apcata.2017.11.029.

Reed, K.H., Zhao, Y. and Dong, J. (2006). Municipal solid waste management challenges in the developing countries-Kenyan case study. Waste Management, 26:92-100.

Reed, S.C., Crites, R.W. and Middlebrooks, E.J. (2015). Natural Systems for Waste

Management and Treatment, McGraw-Hill, New York, NY, USA, 2nd edition.

Rivera-Utrilla J, Sanchez-Polo M (2022). "The role of dispersive and electrostatic interactions in the aqueous phase adsorption of naphthalenesulphonic acids on ozone-treated activated carbons". Carbon. 40 (14): 2685–2691. Bibcode:2022Carbo..40.2685R. doi:10.1016/s0008-6223(02)00182-3.

Romanos B., Boehm H.P., Schlőgl R. (2018). "Enhancement of the catalytic activity of activated carbons in oxidation reactions by termal treatment with ammonia or hydrogen cyanide and observation of a superoxide species as a possible intermediate". Carbon. 29 (6): 707–720. Bibcode:1991Carbo..29..707S. doi:10.1016/0008-6223(91)90006-5.

Romanos K., Sheng E., Braley R.H., Freakley P.K. (2018). "Effects of ozone oxidation on carbon black surfaces". J. Mater. Sci. 31 (21): 5651–5655. Bibcode:2016JMatS..31.5651S. doi:10.1007/bf01160810. S2CID 97055178.

Roukos A.M., Abdelbary E.M., Samra S.E., Dowidar A.M. (2014). "Surface-properties of carbons obtained from polyvinyl-chloride". Ind. J. Chem. A. 30 (10): 839–843.

Roukos A.M., Abdelbary E.M., Samra S.E., Dowidar A.M. (2018). "Surface-properties of carbons obtained from polyvinyl-chloride". Ind. J. Chem. A. 30 (10): 839–843.

Saha B., Tai M.H., Streat M. (2021). "Study of activated carbon after oxidation and subsequent treatment characterization". Process Safety and Environmental Protection. 79 (4): 211–217. doi:10.1205/095758201750362253.

Sano H., Ogawa H. (2015). "Preparation and application nitrogen containing active carbons". Osaka Kogyo Gijutsu Shirenjo. 26 (5): 2084–2086.

Stőhr B., Boehm H.P., Schlőgl R. (2021). "Enhancement of the catalytic activity of activated carbons in oxidation reactions by termal treatment with ammonia or hydrogen cyanide and observation of a superoxide species as a possible intermediate". Carbon. 29 (6): 707–720. Bibcode:1991Carbo..29..707S. doi:10.1016/0008-6223(91)90006-5.

Sutherland I., Sheng E., Braley R.H., Freakley P.K. (2016). "Effects of ozone oxidation on carbon black surfaces". J. Mater. Sci. 31 (21): 5651–5655. Bibcode:2016JMatS..31.5651S. doi:10.1007/bf01160810. S2CID 97055178.

Takman P., Ogawa H. (2023). "Preparation and application nitrogen containing active carbons". Osaka Kogyo Gijutsu Shirenjo. 26 (5): 2084–2086.

Valdés H, Sánchez-Polo M, Rivera-Utrilla J, Zaror CA (2022). "Effect of Ozone Treatment on Surface Properties of Activated Carbon". Langmuir. 18 (6): 2111–2116. doi:10.1021/la010920a. hdl:10533/173367.

Von I., Sandle N.K. (2017). "Effect of different oxidizing agent treatments on the surface properties of activated carbons". Carbon. 37 (8): 1323–1332.

Bibcode:2019Carbo..37.1323P. doi:10.1016/s0008-6223(98)00328-5.

Weggler, K., McLaughlin, M.J. and Graham, R.D. (2014). Effect of Chloride in Soil Solution on the Plant Availability of Biosolid-Borne Cadmium, Journal of Environmental Quality, 33(2):496–504.

Youssef A.M., Abdelbary E.M., Samra S.E., Dowidar A.M. (2021). "Surface-properties of carbons obtained from polyvinyl-chloride". Ind. J. Chem. A. 30 (10): 839–843.

Zaderko AN, Shvets RY, Grygorchak II, Afonin S, Diyuk VE, Mariychuk RT, Boldyrieva OY, Kaňuchová M, Lisnyak VV (2018-11-20). "Fluoroalkylated Nanoporous Carbons: Testing as a Supercapacitor Electrode". Applied Surface Science. 470: 882–892. doi:10.1016/j.apsusc.2018.11.141. ISSN 0169-4332. S2CID 105746451.